# Study of mid-infrared laser action in chalcogenide rare earth doped glass with $Dy^{3+}$, $Pr^{3+}$and $Tb^{3+}$

**Ł. Sójka,[1,2] Z. Tang,[2] H. Zhu,[2] E. Bereś-Pawlik,[1] D. Furniss,[2] A. B. Seddon,[2] T. M. Benson,[2] and S. Sujecki[2,*]**

[1]*Institute of Telecommunication, Teleinformatics & Acoustics, Wroclaw University of Technology, Wybrzeze Wyspianskiego 27, 50-370 Wroclaw, Poland*

[2]*George Green Institute for Electromagnetics Research, University of Nottingham, University Park, NG7 2RD Nottingham, UK*

**slawomir.sujecki@nottingham.ac.uk*

**Abstract:** We present a study of chalcogenide glass fiber lasers doped with $Dy^{3+}$, $Pr^{3+}$ or $Tb^{3+}$ that would operate in the mid-infrared wavelength range. A set of chalcogenide glass samples doped with different concentrations of rare earth ions is fabricated. The modeling parameters are directly extracted from FTIR absorption measurements of the fabricated bulk glass samples using Judd-Ofelt, Füchtbauer–Ladenburg theory and McCumber theory. The modeling results show that, for all the dopants considered, an efficient mid-infrared laser action is possible if optical losses are kept at the level of 1dB/m or below.



**OCIS codes:** (140.3380) Laser materials; (140.0140) Lasers and laser optics; (140.3070) Infrared and far-infrared lasers.

## References and links

1. L. Bachmann, K. Rosa, P. A. da Ana, D. M. Zezell, A. F. Craievich, and G. Kellermann, "Crystalline structure of human enamel irradiated with Er,Cr:YSGG laser," Laser Phys. Lett. **6**(2), 159–162 (2009).
2. H. Jelínková, O. Kőhler, M. Němec, P. Koranda, J. Šulc, V. Kubeček, P. Drlík, M. Miyagi, Y.-W. Shi, Y. Matsuura, M. R. Kokta, P. Hrabal, and M. Jelinek, "Comparison of mid infrared lasers effect on ureter tissue," Laser Phys. Lett. **1**(3), 143–146 (2004).
3. S. Jackson, "Towards high-power mid-infrared emission from a fibre laser," Nat. Photonics **6**(7), 423–431 (2012).
4. A. B. Seddon, Z. Tang, D. Furniss, S. Sujecki, and T. M. Benson, "Progress in rare-earth-doped mid-infrared fiber lasers," Opt. Express **18**(25), 26704–26719 (2010).
5. L. B. Shaw, B. Cole, P. A. Thielen, J. S. Sanghera, and I. D. Aggarwal, "Mid-wave IR and long-wave IR laser potential of rare-earth doped chalcogenide glass fiber," IEEE J. Quantum Electron. **37**(9), 1127–1137 (2001).
6. W. A. King, A. G. Clare, and W. C. Lacourse, "Laboratory preparation of highly pure $As_2Se_{33}$ glass," J. Non-Cryst. Solids **181**(3), 231–237 (1995).
7. E. M. Dianov, V. G. Plotinchenko, Y. N. Pyrkov, I. V. Smolnikov, S. A. Koleskin, G. G. Devyotykh, M. F. Churbanov, G. E. Snopatin, I. V. Skipachev, and R. M. Shaposhnikov, "Single-mode As–S glass fibers," Inorg. Mater. **39**(6), 627–630 (2003).
8. M. F. Churbanov, V. S. Shiryaev, A. I. Suchkov, A. A. Pushkin, V. V. Gerasimenko, R. M. Shaposhnikov, E. M. Dianov, V. G. Plotnichenko, V. V. Koltashev, Y. N. Pyrkov, J. Lucas, and J.-L. Adam, "High-purity As–S–Se and As–Se–Te glasses and optical fibers," Inorg. Mater. **43**(4), 441–447 (2007).
9. G. E. Snopatin, V. S. Shiryaev, V. G. Plotnichenko, E. M. Dianov, and M. F. Churbanov, "High-purity chalcogenide glasses for fiber optics," Inorg. Mater. **45**(13), 1439–1460 (2009).
10. P. Toupin, L. Brilland, J. Trolès, and J. Adam, "Small core Ge-As-Se microstructured optical fiber with single-mode propagation and low optical losses," Opt. Mater. Express **2**(10), 1359–1366 (2012).
11. J. Troles, Y. Niu, C. Duverger-Arfuso, F. Smektala, L. Brilland, V. Nazabal, V. Moizan, F. Desevedavy, and P. Houizot, "Synthesis and characterization of chalcogenide glasses from the system Ga–Ge–Sb–S and preparation of a single-mode fiber at 1.55 µm," Mater. Res. Bull. **43**(4), 976–982 (2008).
12. V. Moizan, V. Nazabal, J. Troles, P. Houizot, J. L. Adam, J. L. Doualan, R. Moncorge, F. Smektala, G. Gadret, S. Pitois, and G. Canat, "$Er^{3+}$-doped GeGaSbS glasses for mid-IR fibre laser application: synthesis and rare earth spectroscopy," Opt. Mater. **31**(1), 39–46 (2008).

#174352 - $15.00 USD Received 16 Aug 2012; revised 4 Oct 2012; accepted 4 Oct 2012; published 17 Oct 2012

13. Z. Tang, N. C. Neate, D. Furniss, S. Sujecki, T. M. Benson, and A. B. Seddon, "Crystallization behavior of $Dy^{3+}$-doped selenide glasses," J. Non-Cryst. Solids **357**(11-13), 2453–2462 (2011).
14. Z. Tang, D. Furniss, S. Sujecki, T. M. Benson, and A. B. Seddon, "The effect of the nature of the rare earth additive on chalcogenide glass stability," Proc. SPIE **7912**, 79121F (2011).
15. R. S. Quimby, L. B. Shaw, J. S. Sanghera, and I. D. Aggarwal, "Modeling of cascade lasing in Dy:chalcogenide glass fiber laser with efficient output at 4.5 μm," IEEE Photon. Technol. Lett. **20**(2), 123–125 (2008).
16. S. Sujecki, L. Sojka, E. Beres-Pawlik, Z. Tang, D. Furniss, A. B. Seddon, and T. M. Benson, "Modelling of a simple $Dy^{3+}$ doped chalcogenide glass fibre laser for mid-infrared light generation," Opt. Quantum Electron. **42**(2), 69–79 (2010).
17. B. M. Walsh, N. P. Barnes, and B. Di Bartolo, "Branching ratios, cross sections, and radiative lifetimes of rare earth ions in solids: application to $Tm^{3+}$ and $Ho^{3+}$ ions in $LiYF_4$," J. Appl. Phys. **83**(5), 2772–2787 (1998).
18. B. R. Judd, "Optical absorption intensities of rare-earth ions," Phys. Rev. **127**(3), 750–761 (1962).
19. G. S. Ofelt, "Intensities of crystal spectra of rare-earth ions," J. Chem. Phys. **37**(3), 511–520 (1962).
20. W. T. Carnall, P. R. Fields, and K. Rajnak, "Spectral intensities of the trivalent lanthanides and actinides in solution. II. $Pm^{3+}$, $Sm^{3+}$, $Eu^{3+}$, $Gd^{3+}$, $Tb^{3+}$, $Dy^{3+}$, and $Ho^{3+}$," J. Chem. Phys. **49**(10), 4412 (1968).
21. H. G. Dantanarayana, A. Vukovic, P. Sewell, Z. G. Lian, D. Furniss, A. B. Seddon, E. A. Romanova, A. Konyukhov, B. Derkowska, J. Orava, T. Wagner, and T. M. Benson, "The optical properties of chalcogenide glasses: from measurement to electromagnetic simulation tools," in Proceedings of the 12th International Conference on Transparent Optical Networks (ICTON 2010), June 27 - July 1 2010, Munich, pp. 1–4.
22. W. B. Fowler and D. L. Dexter, "Relation between absorption and emission probabilities in luminescent centers in ionic solids," Phys. Rev. **128**(5), 2154–2165 (1962).
23. D. E. McCumber, "Einstein relations connecting broadband emission and absorption spectra," Phys. Rev. **136**(4A), A954–A957 (1964).
24. S. D. Jackson, M. Pollnau, and J. Li, "diode pumped erbium cascade fiber lasers," IEEE J. Quantum Electron. **47**(4), 471–478 (2011).
25. B. M. Walsh, "Dual wavelength lasers," Laser Phys. **20**(3), 622–634 (2010).

## 1. Introduction

Mid-infrared light sources are among the most intensively developed photonic devices in recent years. This is because they are needed for many important applications, which include biomedical sensing, environmental monitoring and manufacturing process and quality control *e.g.* product purity in the pharmaceutical industry [1,2]. An ideal mid-infrared light source should be characterized by: small dimensions, simple and robust construction, low price, high efficiency, high output power, broad tuning range and good quality of the output beam. Fiber lasers have demonstrated the ability to meet all these requirements. However, commercially available fiber lasers, including those based on ZBLAN glass, can cover only the wavelength range between 300 nm and 3 μm. A recent review of the progress on ZBLAN glass based MIR fiber laser technology is given in [3]. Achieving longer wavelengths requires primarily the development of suitable lower phonon energy host glass materials so that the lanthanide radiative transitions that correspond to mid-infrared wavelengths are not quenched by the multiphonon transitions [4,5]. One of the candidates to become a host material for the mid-infrared fiber lasers is the chalcogenide glass. Suitable chalcogenide glasses are chemically and mechanically durable, can be drawn into a low loss fiber and doped with lanthanides [4–14]. The feasibility of the mid-infrared fiber laser realization using a chalcogenide glass fiber doped with dysprosium was first demonstrated in [15] and further explored in [16]. The use of dysprosium limits the operating wavelength to about 4.5 μm. In order to access longer wavelengths the use of other lanthanide elements is needed. Therefore, in this paper we study the feasibility of an efficient fiber laser realization in a chalcogenide glass host using $Tb^{3+}$ and $Pr^{3+}$ dopants, and compare the results with those obtained using dysprosium.

## 2. Fabrication and optical characterisation of rare earth doped chalcogenide glasses

GeAsGaSe glasses doped with 500, 1000 and 1500 ppmw (by weight) of $Dy^{3+}$, $Tb^{3+}$ and $Pr^{3+}$ were prepared by the melt-quenching method. High purity elements: Ge, Ga, Se (all 5 N, Cerac); As (7 N, Furukawa Electric Ltd.) and $Dy^3$, $Tb^{3+}$, $Pr^{3+}$ were batched inside a glove-box (≤ 0.1 ppm $O_2$, ≤ 0.1 ppm $H_2O$; MBraun), into a silica glass ampoule (< 1.0 ppm OH, ID/OD = 10 mm/14 mm) which had been air- and vacuum- baked. We have shown in previous work [14] that the most stable rare earth doped chalcogenide glass compositions are those for which

#174352 - $15.00 USD Received 16 Aug 2012; revised 4 Oct 2012; accepted 4 Oct 2012; published 17 Oct 2012

the rare earth has been added in elemental form; here we have added the rare earth (99.9%, Alfa Aesar) as a metal foil in each case (99.9%, Alfa Aesar), added in ppmw to the molar% GeAsGaSe glasses.

The As and Se were further purified by heating under vacuum prior to batching. Batched sample weights were 8–9 g. The ampoule was sealed under vacuum (~$10^{-3}$ Pa), placed in a rocking furnace, heated at 40 °C/h and experienced a 12 h dwell at 850 °C, to achieve homogenization, followed by a 3 h vertical hold for refining as the temperature was decreased at 65 °C/h from 850 °C to 650 °C. The ampoule was quenched through the glass transition temperature first in air (for around 30 seconds) then in a furnace at a temperature close to the glass transition temperature (for around 30 seconds) and then by nitrogen gas (BOC) jet flow. Figure 1a presents a photograph of an example fabricated glass rod. In this case the doping concentration, and the glass composition, was 1000 ppm of $Tb^{3+}$, and $Ge_{16.5}As_{16}Ga_3Se_{64.5}$, respectively.

In order to prepare samples for Fourier Transform Infrared Spectroscopy (FTIR) measurements, 3 mm discs were cut from the as-annealed glass rod, ground using 1000 silicon powder and finally polished using in turn to a 6 µm, 3 µm and 1 µm finish. The polished disc samples were placed in the spectrometer Bruker IFS 66/S sample chamber and purged for around 20 minutes prior to spectral collection. The FTIR spectrometer was purged with dry air (Parker Filtration, FT-IT purge gas generator, 75-52-12VDC) to remove both $CO_2$ and $H_2O$ from the atmosphere. FTIR spectra were collected for the wavelengths range from 0.6 µm to 10 µm. Figure 1b shows a prepared sample ready for the FTIR measurement. This sample had been doped with 1000 ppm of $Tb^{3+}$ into the $Ge_{16.5}As_{16}Ga_3Se_{64.5}$ host glass.

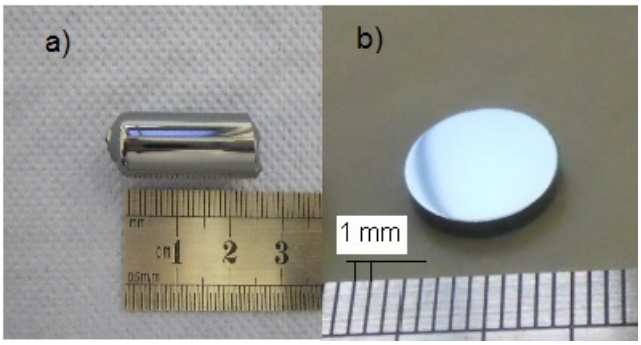


Fig. 1. a) Terbium doped chalcogenide glass rod bulk sample. b) Terbium doped chalcogenide glass sample ready for FTIR measurement.

## 3. Results

In order to extract the Judd-Ofelt parameters, the peak spectral area for the relevant transitions was calculated [17–19]. The absorption area is connected with dipole line strength, $S_{jj'}^{ed}$ by the equation:

$$\int_{band} k(\lambda)d\lambda = \frac{8\pi^3 e^2}{3hc}\frac{N\lambda}{(2J+1)n^2}\left[\frac{n(n^2+2)^2}{9}S_{jj'}^{ed} + n^3 S_{jj'}^{md}\right] \quad (1)$$

where $k(\lambda)$ is the absorption coefficient at wavelength $\lambda$, $e$ is the unit electron charge, $h$ is the Planck's constant, $n$ is the refractive index, $\lambda_{pk}$ is the mean wavelength associated with the transitions, $J$ is the angular quantum number of the initial states, $J'$ is the angular quantum number of the final state and $c$ is the speed of light in free space. The units of $h$, $e$, $c$ should be in cgs (Centimeter-Gram and Second) units.

#174352 - $15.00 USD Received 16 Aug 2012; revised 4 Oct 2012; accepted 4 Oct 2012; published 17 Oct 2012

In order to determine the Judd-Ofelt parameters $\Omega_2$, $\Omega_4$, $\Omega_6$ the electric dipole line strengths were fit by a least squares fit to the values of the reduced matrix elements:

$$S_{JJ'}^{ed} = \sum_{t=2,4,6} \Omega_t \left| \left\langle 4f^n [S,L] J \left\| U^t \right\| 4f^{n'} \left[ S'L' \right] J' \right\rangle \right|^2 \tag{2}$$

$$\Omega = \left( M'M \right)^{-1} M' \cdot S_{jj'}^{ed} \tag{3}$$

$S_{jj'}^{md}$ the magnetic dipole line strength, was calculated from intermediate coupled wavefunctions:

$$S_{jj'}^{md} = \left( \frac{\hbar}{2mc} \right) \left\langle f^n [SL] J \left\| L + 2S \right\| f^{n'} \left[ S'L' \right] J' \right\rangle^2 \tag{4}$$

From the Judd-Ofelt parameters, line strengths were calculated for all transitions and electric dipole and magnetic dipole intermanifold spontaneous emission rates, and were determined by:

$$A_{JJ'}^{ed} = \frac{64\pi^4 e^2}{3h(2J+1)\lambda^3} \frac{n\left(n^2+2\right)^2}{9} S_{JJ'}^{ed} \tag{5}$$

and:

$$A_{JJ'}^{md} = \frac{64\pi^4 e^2}{3h(2J+1)\lambda^3} n^3 S_{JJ'}^{md} \tag{6}$$

The total radiative rate of a manifold is the sum of the intermanifold spontaneous emission rates, or:

$$A_J = \sum_{J'} A_{JJ'} \tag{7}$$

From this, we can define the fluorescence branching ratio as:

$$\beta_{JJ'} = \frac{A_{JJ'}}{A_J} \tag{8}$$

The number of spectral absorption bands that has been used in the Judd-Ofelt computations for $Dy^{3+}$ were used 5 peaks at 0.9, 1.1, 1.3, 1.7, 3.0 μm, for $Pr^{3+}$ were used 5 peaks at 1.5, 1.6, 2.0, 2.3, 4.5 μm and for $Tb^{3+}$ were used 6 peaks at 1.85, 1.9, 2.0, 2.3, 2.9, 4.5 μm. To minimize the error, the measured FTIR spectra were corrected by extracting the baseline function. For each sample three baseline functions were extracted by choosing at least 40 points in the absorption spectrum and fitting the spectra using a polynomial function. This procedure yielded nine sets of Judd-Ofelt parameters. The reduced matrix elements used in these calculations were taken from [20]. The magnetic dipole line strength was calculated from the intermediate coupled wave functions [17]. The values of refractive index were calculated from a Cauchy polynomial, where the polynomial coefficients were obtained by fitting the experimental data [21]. In order to reduce the error resulting from the baseline function extraction an average over all nine sets of Judd-Ofelt parameters was calculated for each dopant. Table 1 shows the calculated Judd-Ofelt parameters for the fabricated chalcogenide glass samples. The calculated Judd-Ofelt parameters are in good agreement with the parameters presented in the literature for doped chalcogenide glasses (albeit with slightly different glass composition) [5]. From the calculated Judd-Ofelt parameters, the radiative

#174352 - $15.00 USD Received 16 Aug 2012; revised 4 Oct 2012; accepted 4 Oct 2012; published 17 Oct 2012

lifetimes and branching ratios were obtained. Table 2 shows the spectroscopic parameters for the relevant transitions.

The absorption cross sections were directly obtained from the FTIR absorption measurements. The emission cross sections were derived from the absorption cross section spectra using the McCumber theory [22,23]. The shape of missing absorption and emission cross sections (for 4 μm $Pr^{3+}$ and 7.5 μm $Tb^{3+}$) were taken from [5] and scaled using lifetime and branching ratio values taken from Table 2. The calculated absorption and emission cross section are shown in Fig. 2.

**Table 1. Calculated Judd-Ofelt parameters for $Ge_{16.5}As_{16}Ga_3Se_{64.5}$ glass doped with $Dy^{3+}$, $Pr^{3+}$ and $Tb^{3+}$**

| | $\Omega_2$ ($10^{-20}$cm$^2$) | $\Omega_4$ ($10^{-20}$ cm$^2$) | $\Omega_6$ ($10^{-20}$cm$^2$) |
|---|---|---|---|
| $Dy^{3+}$ | 8.59 | 2.23 | 2.19 |
| $Pr^{3+}$ | 9.77 | 6.10 | 6.73 |
| $Tb^{3+}$ | 7.63 | 5.79 | 2.21 |

**Table 2. Calculated fluorescence branching ratio and radiative lifetime of $Dy^{3+}$, $Pr^{3+}$ and $Tb^{3+}$, in $Ge_{16.5}As_{16}Ga_3Se_{64.5}$ glass**

| | $Dy^{3+}$ | $Pr^{3+}$ | $Tb^{3+}$ |
|---|---|---|---|
| Concentration | 1000-2000 ppm | 500-1500 ppm | 500-1500 ppm |
| Lifetime of level 3 | 2.2 ms | 2.7 ms | 5.9 ms |
| Lifetime of level 2 | 6.1 ms | 10.3 ms | 11.8 ms |
| Branching ratio for 3-2 transitions | 0.0816 | 0.39 | 0.0876 |
| Pump wavelength | 1.71 μm | 2.04 μm | 2.95 μm |
| Signal wavelength ($\lambda_1$) | 4.6 μm | 4.89 μm | 7.5 μm |
| Idler wavelength ($\lambda_2$) | 3.20 μm | 3.70 μm | 5.1 μm |

#174352 - $15.00 USD Received 16 Aug 2012; revised 4 Oct 2012; accepted 4 Oct 2012; published 17 Oct 2012

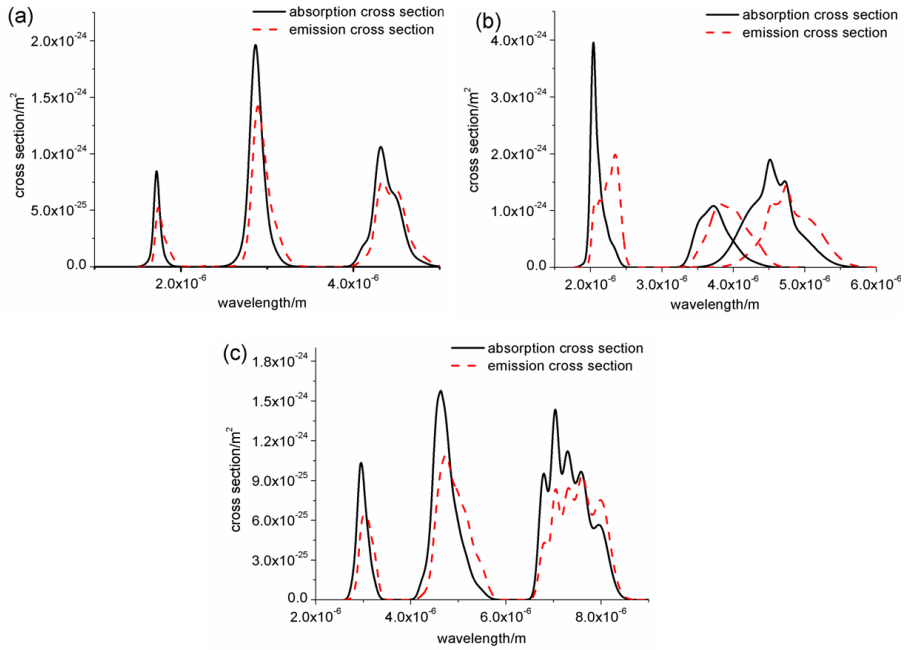


Fig. 2. The spectral dependence of the emission and absorption cross section for a) $Dy^{3+}$ b) $Pr^{3+}$ and c) $Tb^{3+}$.

## 4. Modeling of mid-infrared chalcogenide fiber lasers

Figure 3 shows the energy level diagrams for the 3 lanthanide ion dopants studied. Achieving a mid-infrared laser action in chalcogenide glasses doped using such energy level configurations is not straightforward since both the upper and lower laser levels tend to have long photon decay lifetimes. In order to overcome this difficulty, we apply an appropriate cascade laser configuration. The idea of the cascade configuration consists in adding a laser signal (idler) that depopulates the lower laser level. The cascade lasing configuration also benefits from the fact that the lower level is depopulated radiatively, which reduces the amount of heat generated. The cascade chalcogenide glass laser configuration is discussed in detail in [15,16,24,25].

The numerical model used here was based on solving self-consistently the level population rate equations and optical propagation equations [16]. The fiber structure assumed is a double-clad one with a single mode (for the signal and idler wavelengths), core with a radius of 5.5 μm and a multimode clad with a radius of 30 μm for the pump wavelength. The feasibility of fabrication of single mode chalcogenide glass fibers was demonstrated in [9–14]. The pump confinement factor was calculated under the assumption that the pump power is uniformly distributed in the fiber cladding. The confinement factors for the signal and the idler were calculated using the mode field distribution obtained at the nominal wavelengths (Table 2). A fiber laser resonator structure consists of two pairs of fiber Bragg gratings (FBG). One pair of gratings traps the signal, while the other one confines the idler. The reflectivity of the input FBG for the pump wavelength is 0.05 while for the signal and the idler it is 0.95. The output reflectivity is 0.05 for the signal and 0.9 for the idler. The level of losses assumed for all the wavelengths (at the pump and emissions' wavelengths) is 1 dB/m. (We note that in a number of papers much lower loss levels have been demonstrated experimentally for some chalcogenide glass fibers of simple composition [9].) The remaining modeling parameters are presented in Table 2 and Fig. 2.

#174352 - $15.00 USD Received 16 Aug 2012; revised 4 Oct 2012; accepted 4 Oct 2012; published 17 Oct 2012

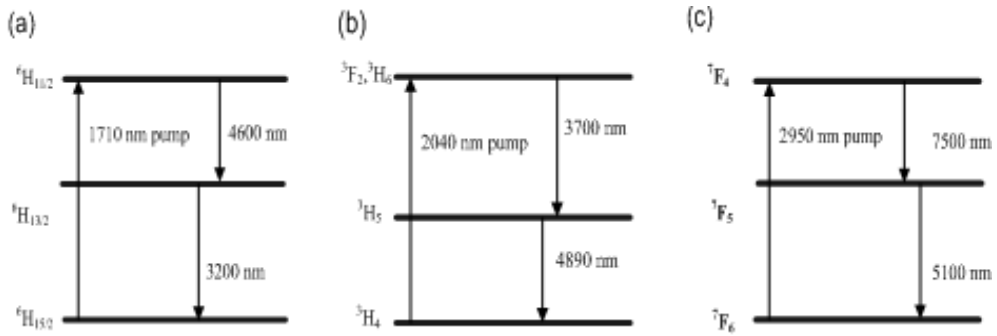


Fig. 3. Simplified energy level diagram showing cascade laser transitions of a) $Dy^{3+}$ b) $Pr^{3+}$ and c) $Tb^{3+}$ to the ground state.

We consider first the chalcogenide glass doped with $Dy^{3+}$. The relevant energy level diagram is presented in Fig. 3a. The doping level is equal to 1500 ppmw. (For this doping level fabricated chalcogenide glass bulk samples show no signs of crystallization after melt-cooling and annealing [13].) The laser action at 4.6 μm in $Dy^{3+}$ doped glass can be obtained between the $H_{11/2}$ and $H_{13/2}$ levels by pumping directly the level $H_{11/2}$ by a 1.71 μm pump. The idler wavelength (levels $H_{13/2}$ and $H_{15/2}$) is set to 3.2 μm. Figure 4a shows the dependence of idler and signal power on the fiber length and pump power. The slope efficiency for 4.6 μm wavelength reaches about 9%, which agrees with the results presented in [15,16].

The second dopant considered is praseodymium, $Pr^{3+}$. $Pr^{3+}$ has strong absorption bands at 1.55 μm and 2 μm. Here the band at 2 μm is used for the pumping. The main problem with pumping with a light source at 2 μm in $Pr^{3+}$ doped chalcogenide glass is that the level $F_2$-$H_6$ has a long lifetime, of about 2.7 ms. In order to de-excite the level $F_2$-$H_6$ faster we propose using a cascade laser structure. We therefore fix the FBG wavelengths for the signal and the idler at 4.89 μm and 3.7 μm, respectively. Figure 4b shows the dependence of the idler and signal power on the fiber length and the pump power. The slope efficiency for 4.89 μm wavelength reaches about 16%. The main reason why this efficiency is much higher than for $Dy^{3+}$ is the fact that the absorption cross section at 2.04 μm is four times larger than that for $Dy^{3+}$ (at 1.71 μm). This allows the pump power to be absorbed much quicker and be less affected by the fiber losses.

The last fiber laser considered is based on chalcogenide glass doped with terbium, $Tb^{3+}$. The main advantage of terbium is the possibility of obtaining laser action at 7.5 μm. This is the longest wavelength emission ever studied in lanthanide-doped chalcogenide glasses. The simplified energy level diagram of $Tb^{3+}$ is presented in Fig. 3c. In this case the laser action at 7.5 μm occurs between the levels $^7F_4$ and $^7F_5$, while the idler operates at 5.1 μm (between levels $^7F_5$ and $^7F_6$). The pump wavelength that we assumed in our calculation is 2.95 μm and is covered by commercial available Er:YAG lasers and also by $Er^{3+}$ and $Ho^{3+}$ doped ZBLAN fiber lasers [24]. The fiber structure and resonator parameters are the same as in the previous cases. Figure 4c shows the dependence of idler and signal power on the fiber length and the pump power. The results confirm that the efficient laser action at 7.5 μm is possible with the slope efficiency reaching about 9%. These results indicate that $Tb^{3+}$ doped chalcogenide glass is a good candidate for the construction of a first fiber laser operating at 7.5 μm wavelength.

#174352 - $15.00 USD Received 16 Aug 2012; revised 4 Oct 2012; accepted 4 Oct 2012; published 17 Oct 2012

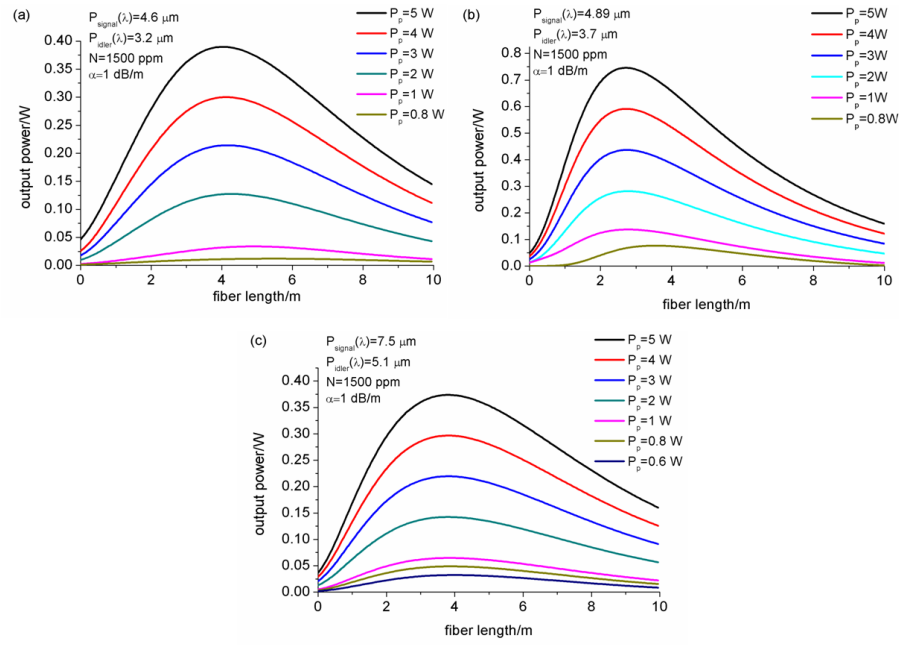


Fig. 4. Calculated dependence of the output signal power on the fiber length with different pump power for a) $Dy^{3+}$ b) $Pr^{3+}$ and c) $Tb^{3+}$.

Figure 5 shows the dependence of the output power on the length for selected values of the fiber loss. In all cases the doping concentration is 1500 ppmw and the pump power equals 5 W. This study shows that significant output power can be achieved even with losses as high as 3 dB/m.

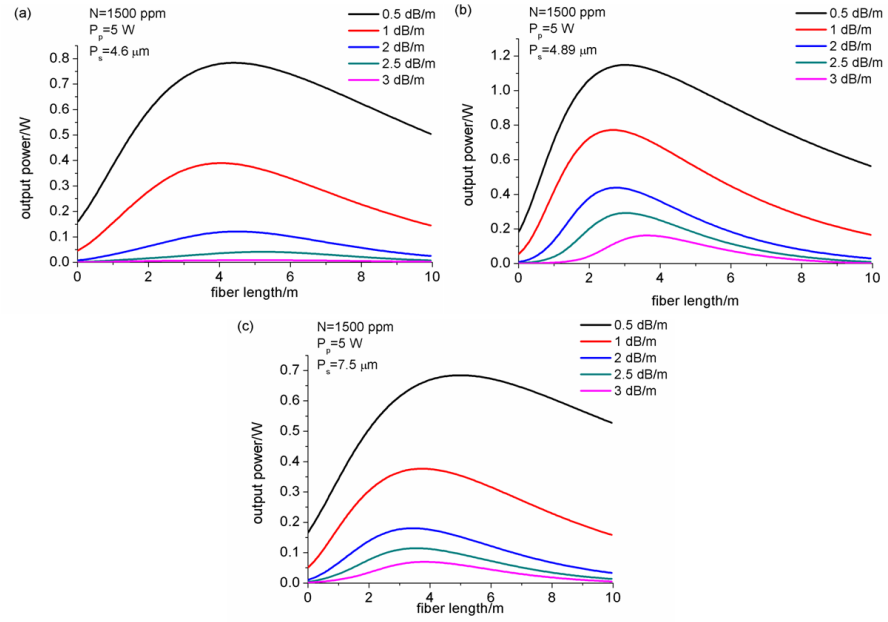


Fig. 5. Calculated dependence of the output signal power on the fiber length with different levels of fiber optical losses for a) $Dy^{3+}$ b) $Pr^{3+}$ c) $Tb^{3+}$.

#174352 - $15.00 USD Received 16 Aug 2012; revised 4 Oct 2012; accepted 4 Oct 2012; published 17 Oct 2012

## 5. Summary

In this paper the possibility of realizing a mid-infrared laser based on rare earth doped chalcogenide glass fibers was investigated. A set of chalcogenide glass samples doped with $Dy^{3+}$, $Pr^{3+}$ and $Tb^{3+}$ was fabricated. Based on the experimental results and numerical modeling, the feasibility of lasing in chalcogenide glasses doped with $Dy^{3+}$, $Pr^{3+}$ and $Tb^{3+}$ was studied. The results of numerical modeling show that in all considered cases an efficient laser action at 4.6 μm, 4.89 μm and 7.5 μm respectively with pumping at 1.71 μm, 2.04 μm and 2.95 μm (efficiency about 8%-16%) in the cascade configuration can be achieved if the fiber losses are brought down to 1 dB/m level.

#174352 - $15.00 USD Received 16 Aug 2012; revised 4 Oct 2012; accepted 4 Oct 2012; published 17 Oct 2012